High-pressure and temperature ammonia flame speeds

Alka Karan, Guillaume Dayma, Christian Chauveau, Fabien Halter

13th Asia-Pacific Conference on Combustion 2021
ADNEC, Abu Dhabi – UAE
4 – 9 December 2021

High-pressure and temperature ammonia flame speeds

Alka Karan[1], Guillaume Dayma[1, 2], Christian Chauveau[1], Fabien Halter[1, 2]

[1]ICARE-CNRS

1C avenue de la Recherche Scientifique, Orléans, 45071, France

[2]Université d'Orléans

Château de la Source, avenue du Parc Floral, Orléans, 45067, France

Abstract

The use of ammonia as an alternative fuel in gas turbines or spark-ignition engines have already been tested. As high pressures and temperatures are reached in these industrial combustors, it is necessary to obtain a robust detailed kinetic mechanism able to predict laminar flame speed for ammonia at these conditions. In order to assess the validity of such a kinetic mechanism, reliable targets are mandatory. The present study focusses on measuring flame speeds at elevated thermodynamic conditions for different equivalence ratios in a constant volume spherical chamber. This new methodology allows to provide 3D maps of S_L = f (*p, T*) for different equivalence ratios. A literature study was also performed to evaluate and select the most recent kinetic mechanisms for ammonia combustion under these extreme conditions. Sensitivity analyses highlighting the key reactions for two of the most promising mechanisms has been performed. Interestingly, it turns out that, although they are both in good agreement with our new experimental data, the sensitive reactions are not all the same, indicating the chemistry of ammonia needs further investigations.

1 Introduction

Ammonia has received recent interests as it is carbon-free and relatively safe to store and transport. The use of ammonia as an alternative fuel in combustors like gas turbines [1] and especially in spark-ignition engines [2] has already been tested. Ammonia flames are characterized by a low combustion intensity, low laminar burning velocities and narrow flammability limits. Flame speeds of ammonia in air under stoichiometric conditions are as low as 7 cm s^{-1} at standard atmospheric conditions [3] The low heating value (LHV) of ammonia is 18.8 MJ kg^{-1} which is lower than most of the commonly used fuels like hydrogen and methane [4]. Nevertheless, ammonia is favored in spark-ignition engines as it has a high-octane number. It has an energy density of 22.5 MJ kg^{-1} and can be stored in liquid form under 0.8 MPa at atmospheric temperature [5]. Ammonia is mainly produced by the Haber-Bosch process which is the most economical way to have mass productions. This process can be made carbon-free to make ammonia a true green fuel. Hydrogen is obtained from the electrolysis of water with the help of solar or wind energy (renewable sources of energy) whereas nitrogen is obtained from air filtration.

The adiabatic flame temperature and the auto-ignition temperature of ammonia are at 1800 °C and 650 °C respectively making it a potential contender among other green fuels due to its anti-knock characteristics. In addition, the flammability limit [3] of ammonia (φ = 0.63-1.4) compared to hydrogen (φ = 0.1-7.1) is quite low which makes it safer to store and transport but at the same time difficult to ignite. The low speed of ammonia/air flames [6, 7] leads to an early blow-off and a difficulty in ignition. Ammonia is often combined with hydrogen or methane to increase the overall performance like the flame speeds, flammability limits and power output. Literature is available on different conditions for the combined fuel mixture [4, 8]. Data at high pressure and high temperature are available for ammonia mixed with hydrogen or methane [4, 9-12]. However, for pure ammonia combustion, analyses have been made for a narrow range of pressure (< 10 bar) and temperature (< 473 K) conditions for different equivalence ratios [7, 12]. As high pressures and high temperatures conditions are encountered in spark-ignition engines and gas turbines, it is essential to accurately measure flame speed data for these conditions.

The present study focusses on performing experiments at high temperatures and pressures conditions for different equivalence ratios in a constant volume condition. The results of these experiments provide laminar flame speeds for a pressure range of 2 to 20 bar and a temperature range of 366 to 485 K at 3 different equivalence ratios (i.e. 0.8 / 1.1 / 1.3). 3D maps of S_L = f (*p, T*) for different equivalence ratios can then be generated from this set of experimental data following the expression proposed by [13]. These experimental results are further used to assess the most recent chemical kinetic mechanisms available in the literature under these conditions. Key reactions involved in the pressure and temperature dependence of the flame speed have been identified.

2 Methodology

2.1 Experimental set-up

The experiments were performed in the OPTIPRIME facility of ICARE-CNRS, Orleans, France. This experimental set-up has been already been described [14, 15]. Briefly, from rather low initial pressures and temperatures, a spherical flame outwardly propagating in a constant volume chamber allows reaching high pressures and temperatures assuming an isentropic compression. The 360 ° fused silica ring allows tracking the

Corresponding author. Fax: +33-238-696-004
E-mail address: guillaume.dayma@cnrs-orleans.fr

flame front from the ignition point at the center of the chamber up to the wall where the flame propagates and finally extinguishes. The idea behind the vast visibility range is to be certain that the flame front remains spherical throughout the process without being influenced by gravity effects or hydrodynamic and thermo-diffusive instabilities. The flame speed determination method accounts for the radiation heat losses [15]. The apparatus also consists of a K-type thermocouple to measure the initial temperature and two pressure transducers (AVL GU21D) to measure the pressure simultaneously with the flame radius evolution captured at the rate of 12000 fps using a CMOS camera (PHANTOM V1611).

2.2 Experimental conditions

Experiments were performed for mixtures of NH_3 / O_2 (+Ar, He) at 3 different equivalence ratios: 0.8, 1.1 and 1.3 at an initial temperature of 300 K. For the rich mixtures, the initial pressure ranged between 1 and 4 bar whereas for the lean mixture, it was at 1 bar and 2 bar. It is well-known that these flames are quite unstable in nature so combination of argon and helium was used to stabilize the flame. The ratio of the diluent was chosen such that the mixture could be readily ignited and the flame sustains till it hits the wall. It is difficult to ignite mixtures with a high helium content at low pressures as helium possesses a high thermal diffusivity. In the case of the high-pressure conditions, bigger instabilities are incurred and so, a large percentage of helium is required to stabilize the flame. 30 % of the oxidizer mixture constitutes of oxygen and the remaining 70 % is the diluent for all the conditions. The initial conditions used are represented in the Table 1.

φ	p_0 (bar)	O_2 / diluent
0.8	1	30% O_2 / 49% Ar / 21% He
0.8	2	30% O_2 / 49% Ar / 21% He
1.1	1	30% O_2 / 49% Ar / 21% He
1.1	2	30% O_2 / 49% Ar / 21% He
1.1	1	30% O_2 / 21% Ar / 49% He
1.1	2	30% O_2 / 21% Ar / 49% He
1.1	3	30% O_2 / 21% Ar / 49% He
1.1	4	30% O_2 / 70% He
1.3	1	30% O_2 / 49% Ar / 21% He
1.3	2	30% O_2 / 49% Ar / 21% He
1.3	2	30% O_2 / 21% Ar / 49% He
1.3	3	30% O_2 / 21% Ar / 49% He
1.3	4	30% O_2 / 21% Ar / 49% He
1.3	4	30% O_2 / 70% He

Table 1: Initial conditions used in this work.

The flame speed was calculated using the derivatives of the obtained radius at the corresponding pressure by (1):

$$S_u = \frac{dR_f}{dt} - \frac{\left(R_0^3 - R_f^3\right)}{3\gamma_u R_f^2 p}\frac{dp}{dt} \quad (1)$$

where R_f and R_0 represent the flame radius and the inner chamber radius respectively and γ_u is the heat capacity ratio of the unburnt gas.

2.3 Chemical kinetic mechanisms

The most recent kinetic mechanisms were selected and are represented in the Table 2. On performing this literature review, it was noticed that Okafor [16] gave the most congruent results for lean mixtures and Klippenstein [17] and Zhang [18] gave the best results for the rich mixtures. Konnov [19] and Mathieu [20] seem to over-estimate and under-estimate the flame speeds respectively when compared to the experimental data [3]. The present experimental results were simulated using the premixed laminar flame speed calculator available in Chemkin-Pro [21]. Calculations were performed at GRAD and CURV down to 0.01, selecting Soret effect and the full multi-component formulation to determine species ordinary diffusion coefficients. Under these conditions, ca. 1500 meshes are reached allowing an uncertainty < 1% on the calculated flame speed. Sensitivity analyses on the flow rate were also performed for a few mechanisms to understand the role of the key reactions on the flame speed.

Kinetic Mechanisms	Species	Reactions	Ref.
Klippenstein[a]	33	211	[17]
Dagaut[a]	26	133	[22]
Zhang	37	229	[18]
Shrestha	34	261	[23]
Nakamura	38	232	[24]
Okafor[b]	60	359	[16]
Otomo	32	213	[25]
Stagni	31	203	[26]
Mathieu[a]	33	159	[20]

a. These mechanisms originally include C based compounds which were removed in order to make the calculations faster.

b. The Okafor mechanism was modified to add helium using the third body coefficients of argon when necessary.

Table 2: Chemical kinetic mechanisms tested in this work.

3 Results and discussion

3.1 Experimental and numerical flame speeds

The experiments were performed in the isochoric condition. The isochoric method allows to evaluate a wide range of flame speed data at elevated conditions. The available range for the measurement has been chosen such that the stretch effects that occur in the initial phase and the heat losses endured when the flame front comes very close to the wall do not affect the propagation of the flame front and hence, the flame speed. It is assumed that the temperature of fresh gases evolves isentropically while the flame front propagates. A relative accuracy of less than 0.5% on the flame radius was propagated on the flame speed leading to a maximal error lower than 5% [15]. The experiment traces have been widened to account for this uncertainty.

Among the 9 chosen mechanisms, it was seen that 2 of them, namely Nakamura [24] and Stagni [26], predicted the experimental results at all conditions better than the other mechanisms. Although, the 9 chosen mechanisms could aptly produce the trend, i.e. the flame speed increases with an isentropic increase of temperature and pressure for all the test conditions; there is a variation in the absolute flame speed values. Generally, it was seen that the schemes of Klippenstein [17], Zhang [18] and Dagaut [22] over-estimate the flame speeds when compared to the experimental flame speed whereas Mathieu [20] and Otomo [25] under-estimate the flame speed. The other 4 mechanisms more or less fall within ± 5% error bar of the experimental results. Out of the 14 conditions of this study, three of them are represented here in Figures 1, 2 and 3. These selected conditions represent a slightly fuel-rich (φ = 1.1) condition at three initial pressures (1, 2, and 3 bar) to illustrate the above-mentioned capabilities of the method.

Figure 1 represents the flame speeds at φ = 1.1, T_0 = 300 K, p_0 = 1, 2, and 3 bar as a function of *p* and *T*. These three cases use the same diluent mixture: 49% He and 21% Ar. The experimental data are the blue, red, and green thick lines in the volume. The blue, red, and green thin lines on the lower plane are the projections of these experimental data on the (*p*, T) plane. They represent the isentropic evolution of pressure and temperature starting from each initial condition. The S_L = f (*p*, *T*) map is generated after the formulation (2) proposed by [13] to fit our experimental results under these conditions. Such a map can be generated for each mixture composition (equivalence ratio, nature of the diluent, dilution rate).

$$S_u = S_{u0}\left(\frac{T}{T_0}\right)^{xT+y}\left(\frac{p}{p_0}\right)^{aexp\left(\frac{-p}{b}\right)+c} \quad (2)$$

Under the conditions of Fig. 1, our experimental data are best reproduced using $x = 1.65\times10^{-3}$, y = 1.673, a = 0.742, b = 0.112, c = -0.171.

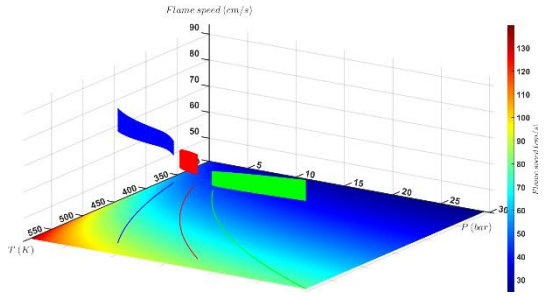

Figure 1: Experimental flame speeds of NH_3/O_2/He/Ar mixtures at φ = 1.1, T_0 = 300 K, p_0 = 1 (blue), 2 (red), and 3 bar (green).

As illustrated by the Figure 2, on analyzing all the cases, it was concluded that both Nakamura and Stagni mechanisms can predict the flame speed closest to the experimental values, that from Nakamura being more difficult to converge.

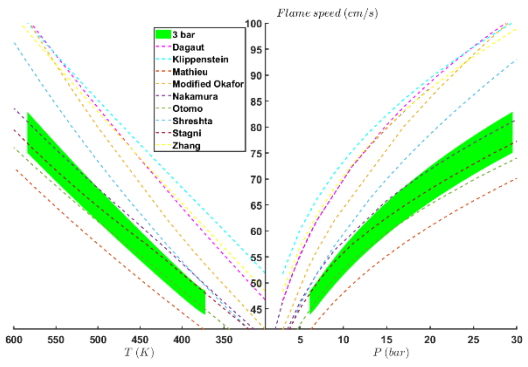

Figure 2: Comparison of experimental flame speeds of NH_3/O_2/He/Ar mixtures at φ = 1.1, T_0 = 300 K, p_0 = 3 bar with different kinetic mechanisms.

3.2 Sensitivity analyses

Sensitivity analyses on the flow rate were performed on a few mechanisms to understand the behavior and to highlight the key reactions. It was seen that the most dominant reaction irrespective of the mechanism and the initial conditions is H + O_2 ⇌ OH + O. It is interesting to note that the sensitivity coefficient on the flow rate for the reactions for all the mechanisms are quite different even though the rate constants are quite similar, indicating that the other rate constants impact the sensitivity of each reactions. On comparing the rate constants of H + O_2 ⇌ OH + O for Klippenstein [17] and Nakamura [24] and the flame speeds it can be confirmed that the discrepancy in the magnitude of flame speeds does not arise from the small difference in values of this k. The vast difference in the flame speeds for different mechanisms may be attributed to the global summation effect of those reactions that do not fall under the top 10 important reactions (11 indeed because the reactions are different depending on the conditions). Since, Nakamura [24] and Stagni [26] estimate the flame speeds closer to the experimental results, a deeper study has been conducted on them.

Figures 3 (a, b) depicts the sensitivity analyses for Nakamura [24] and Stagni [26] mechanisms at φ = 1.1 for an initial pressure of 1 bar and a diluent mixture of 49% He and 21% Ar respectively. The analyses illustrate the similarities but also the differences between both mechanisms in terms of reactions involved as well as magnitude of their sensitivity. It is interesting to note that even though the flame speed predicted by both of these mechanisms are quite close, the top 10 important reactions are not exactly the same. They have 9 reactions in common, the dissociation of HNO being pressure-dependent in Nakamura. It is noticed that the reaction H_2 + O ⇌ H + OH exists within the top 10 important reactions in all cases for both the mechanisms except for the lean cases of Nakamura [24] (not reported here).

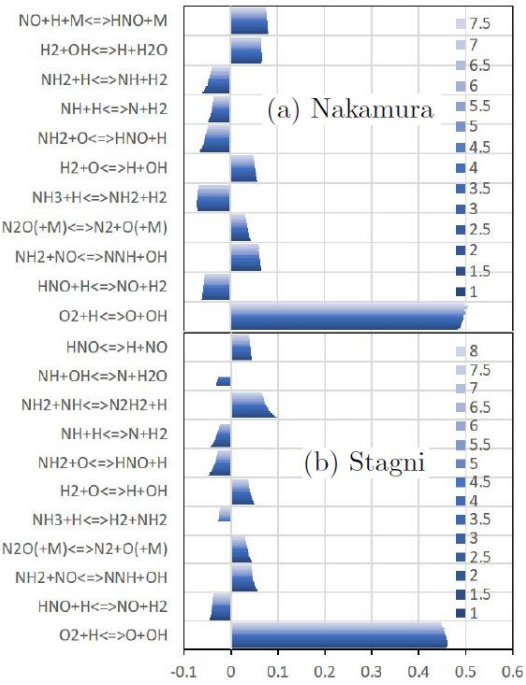

Figure 3: Sensitivity analyses on the flow rate at p_0 = 1 bar, φ = 1.1, 49% He and 21% Ar.

A standard set of reactions is noted for each equivalence ratio apart from the above stated common reactions irrespective of the initial pressure except for H + O_2 (+M) ⇌ HO_2 (+M) which is found only for those with an initial pressure of 2 bar or more. However, none of the stated reactions play a role as significant as the H + O_2 ⇌ O + OH reaction does. Also, from the sensitivity analyses it can be seen that the flame speed is not highly sensitive to pressure. These mechanisms predict a weak dependence of flame speed on pressure. On comparing with methane flames, it is seen that for methane flames [15], the

recombination reaction, $CH_3 + H (+M) \rightleftharpoons CH_4 (+M)$ is one of the main reactions which becomes more sensitive at higher pressure and equivalence ratio. The H radicals produced in the methane flames are consumed at high pressure and so the total reactivity decreases leading to a decrease of flame speed as the pressure increases. The equivalent recombination reaction in the ammonia flames is not sensitive like in methane flames. The dominance of the driving reaction whose rate constant is pressure-independent and the absence of the equivalent sensitive recombination reaction can possibly explain the ability of all the mechanisms to produce the experimental trend invariably.

4 Conclusions

Experiments to measure flame speeds corresponding to the conditions encountered in spark-ignition engines and gas turbines have been performed. The study was done for 3 different equivalence ratios: 0.8,1.1 and 1.3 at an initial temperature of 300 K and an initial pressure ranging from 1 to 4 bar. The data available in the literature gives the flame speeds for a maximum pressure of 5 bar and a temperature of 473 K. From this study, the laminar flame speeds for a pressure of nearly 30 bar and a temperature of 585 K have been obtained. These tests were performed in constant volume condition which is the most efficient way to obtain a wide range of data for elevated conditions. A literature study had been made to select the most recent kinetic mechanisms for ammonia combustion. The flame speeds calculated from these mechanisms have compared to the experiments. It was seen that the chosen mechanisms could produce the experimental trend- increase of flame speed with an isentropic increase of pressure and temperature for all the conditions. On performing a sensitivity analyses, it was understood that the most dominant reaction is $H + O_2 \rightleftharpoons O + OH$. Despite the high sensitivity of this reaction and the rate constant of this reaction being similar for all mechanisms, only 4 mechanisms: Shrestha [23], Nakamura [24], Okafor [16] and Stagni [26] could predict the flame speeds with the ± 5% error bar of the experimental flame speeds. The recombination reaction of the ammonia flames was found to be pressure insensitive. In order to understand the working of the mechanisms, various simulations were performed at isobaric and isothermal conditions. The results of these simulations prove that the mechanisms are temperature-driven and not pressure-driven as the change in flame speed for a small increase in temperature is much higher than the change in flame speed obtained from the same increase in pressure. The maximum influence of pressure is seen only from 1-5 bar after which the flame speeds do not vary a lot. The increase in the flame speed is attributed only to the increase of temperature which promotes the chemical reactivity. The impact of adding the bath gases has been noted for some of the mechanisms. The change in the flame speed response to pressure for Shrestha [23] seems to have a lesser effect from the bath gases composition whereas Stagni [26] and Nakamura [24] seem to be influenced by the constituents of the bath gases.

It can be concluded that the performance of oxy-ammonia flames is in par with the conventional fuels and has a promising future. Ammonia being a non-carbon-based fuel, indeed has the potential to replace the hydrocarbon fuels without a large compromise in performance.

5 Acknowledgment

Put acknowledgements here.

References

[1] A. Valera-Medina, D. Pugh, P. Marsh, G. Bulat, P. Bowen, Int. J. of Hydrogen Energy 42 (2017) 24495-24503.

[2] S. Frigo, R. Gentili, Int. J. of Hydrogen Energy 38 (2013) 1607-1615.

[3] H. Kobayashi, A. Hayakawa, K. K. A. Somarathne, E. C. Okafor, Proc. Combust. Inst. 37(1) (2019) 109-133.

[4] C. Lhuillier, P. Bréquigny, N. Lamoureux, F. Contino, C. Mounaïm-Rousselle, Fuel 263 (2020) 116653.

[5] A. Valera-Medina, H. Xiao, M. Owen-Jones, W. David, P. Bowen, Prog. Energy Combust. Sci. 69 (2018) 63-102.

[6] X. Han, Z. Wang, M. Costa, Z. Sun, Y. He, K. Cen, Combust. Flame 206 (2019) 214-226.

[7] A. Hayakawa, T. Goto, R. Mimoto, Y. Arakawa, T. Kudo, H. Kobayashi, Fuel 159 (2015) 98-106.

[8] C. Mørch, A. Bjerre, M. Gøttrup, S. Sorenson, J. Schramm, Fuel 90 (2011) 854-864.

[9] C. Duynslaegher, H. Jeanmart, J. Vandooren, Fuel 89 (2010) 3540-3545.

[10] A. Goldmann F. Dinkelacker, Fuel 224 (2018) 366-378.

[11] J. Li, H. Huang, N. Kobayashi, Z. He, Y. Nagai, Int. J. Energy Res. 38 (2014) 1214-1223.

[12] K. P. Shrestha, C. Lhuillier, A. A. Barbosa, P. Bréquigny, F. Contino, C. Mounaïm-Rousselle, L. Seidel, F. Mauss, Proc. Combust.Inst. 38(2) (2021) 2163-2174.

[13] E. Hu, X. Li, X. Meng, Y. Chen, Y. Cheng, Y. Xie, Z. Huang, Fuel 158 (2015) 1-10.

[14] F. Halter, Z. Chen, G. Dayma, C. Bariki, Y. Wang, P. Dagaut, C. Chauveau, Combust. Flame 212 (2020) 165-176.

[15] F. Halter, G. Dayma, Z. Serinyel, P. Dagaut, C. Chauveau, Proc. Combust. Inst. 38(2) (2021) 2449-2457.

[16] E. C. Okafor, Y. Naito, S. Colson, A. Ichikawa, T. Kudo, A. Hayakawa, H. Kobayashi, Combust. Flame 204 (2019) 162-175.

[17] S. J. Klippenstein, M. Pfeifle, A. W. Jasper, P. Glarborg, Combust. Flame 195 (2018) 3-17.

[18] Y. Zhang, O. Mathieu, E. L. Petersen, G. Bourque, H. J. Curran, Combust. Flame 182 (2017) 122-141.

[19] A. Konnov, Combust. Flame 156 (2009) 2093-2105.

[20] O. Mathieu, E. L. Petersen, Combust. Flame, 162 (2015) 554-570.

[21] ANSYS CHEMKIN 20.0, ANSYS Reaction Design: San Diego, 2020.

[22] P. Dagaut, P. Glarborg, M. Alzueta, Prog. Energy Combust. Sci. 34 (2008) 1-46.

[23] K. P. Shrestha, L. Seidel, T. Zeuch, F. Mauss, Energy and Fuels, 32 (2018) 10202-10217.

[24] H. Nakamura, S. Hasegawa, Proc. Combust. Inst. 36 (2017) 4217-4226.

[25] J. Otomo, M. Koshi, T. Mitsumori, H. Iwasaki, K. Yamada, Int. J. Hydrogen Energy 43 (2018) 3004-3014.

[26] A. Stagni, C. Cavallotti, S. Arunthanayothin, Y. Song, O.

Herbinet, F. Battin-Leclerc, T. Faravelli, Chem. Eng. 5(4) (2020)
696-711.